Inspection Path Planning of Mobile Communication Base Stations Based on Automatic UAV Nest

Haotian Wu*
School of Telecommunication Engineering, Xidian University, Xi'an, China
*Corresponding author: 22012100029@stu.xidian.edu.cn

Abstract. With the development of 5G mobile networks, the number of mobile communication base stations in China has increased rapidly, and regular inspection and maintenance are required. Traditional manual inspection has some shortcomings and limitations. In recent years, the development of drones and drone nest technology has made drone inspection feasible. Since the automation level of traditional manually controlled drone inspection is low, this paper proposes a base station inspection scheme based on drone nests. By establishing an inspection model and using the simulated annealing algorithm to solve the TSP problem, the drone inspection path is planned to improve the inspection efficiency and the unmanned and automated inspection level. In this paper, the simulation experimental results show that the algorithm can effectively obtain the global optimal solution in a relatively short time, realize the path planning of drone automatic inspection of base stations, and effectively improve the inspection efficiency of drones.

Keywords: Drone nest; automatic inspection; drone path planning; simulated annealing algorithm.

1. Introduction

Base stations are critical to mobile communication networks, enabling wireless signal transmission between wired networks and mobile devices. With the rapid expansion of 5G networks, China's mobile base stations have surged to 11.62 million by the end of 2023, including 6.29 million 4G and 3.38 million 5G stations, representing 29.1% of the total, up 7.8 percentage points from the previous year [1][2].

The stable operation of base stations is crucial for mobile network performance but can be compromised by environmental factors like lightning, acid rain, and bird nesting. Therefore, regular inspection and maintenance are necessary for the operation of base stations. Communication base stations are usually tens of meters high. Traditional inspection methods require professionals to climb to the target point for inspection and maintenance. These methods are not only costly and inefficient, but also difficult to inspect and repair, and there are high safety risks. Moreover, they are restricted by environmental and weather factors and cannot operate normally. Some base stations are located in complex or remote areas, such as mountainous regions, which are hard for conventional vehicles to access. Dispatching personnel to these sites for inspections is time-consuming, labor-intensive, and poses safety risks. In recent years, multi-rotor drones, with their small size, vertical takeoff and landing capabilities, operational flexibility, and ability to carry various inspection equipment, have become a feasible option for unmanned inspections. These drones can quickly reach base stations, capture high-precision images and data, and significantly enhance inspection efficiency and coverage, particularly in remote areas. Moreover, drone inspections help avoid the environmental impact and damage to surrounding vegetation that can occur with manual inspections of remote base stations. As an automated drone docking and charging system, Drone Nest can realize autonomous take-off and landing, charging and data transmission of drones. By equipping remote base stations with drone nests, unmanned remote and efficient autonomous inspections can be achieved around the clock. Additionally, efficient drone path planning can shorten inspection routes, reduce inspection time, and improve overall efficiency. This optimization also lowers energy consumption and increases inspection coverage, which is crucial for widely distributed base stations.

At present, the research on drone inspection path planning has achieved fruitful results in many industries. For example, in the field of wind turbine inspection, Li proposed a hybrid genetic simulated annealing algorithm to solve the TSP problem and obtain the optimal inspection-free path [3]. Cui, Zhang, Ma et al. designed to use multi-rotor drones to inspect power towers and fixed-wing drones to inspect power grids, and used genetic algorithms and genetic simulated annealing (GSA) algorithms to obtain the optimal inspection path [4]. Numerous studies have explored the use of drone nests in various industries, including power inspections, oil and gas pipeline monitoring, and environmental monitoring [5-7]. These applications have greatly improved the automation of drone inspection.

In the current industry practice of drone-based station inspections, manual control by professionals is typically required, limiting automation and preventing autonomous inspections. For instance, Gao mentions a mobile tool vehicle that carries a drone for base station inspections [8]. Therefore, to solve this problem, this paper proposes a solution for drone inspection base stations using drone automatic nesting technology. The proposed approach involves establishing a base station inspection scenario model and designing algorithms to optimize and plan inspection paths. The aim of the solution is to enhance the efficiency of base station inspections and significantly improve the level of automation and unmanned operation.

2. Inspection Plan Design

2.1. Model Construction

The drone needs to inspect at a certain distance from the target point and is constrained by the field of view, so a rectangular detection area will be generated around the target point. The drone detects and scans the target by carrying sensors or cameras, and the constraints on the detection area are shown in Figure 1.

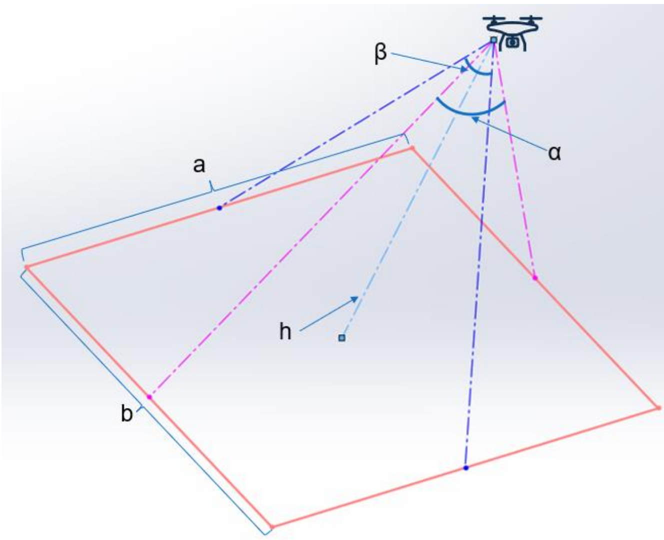

Figure. 1 Constraints of the field of view on the detection area

In the figure, a and b are the length and width of the detected area, h is the vertical distance between the drone and the center of the area, and α and β are the horizontal and vertical field of view of the drone, respectively. The mathematical relationship is as follows:

$$a = 2h \tan\left(\frac{\alpha}{2}\right) \tag{1}$$

$$b = 2h \tan\left(\frac{\beta}{2}\right) \tag{2}$$

The effective detection area S

$$S = a \cdot b \tag{3}$$

For cylindrical base stations, different parts of the base station are divided into independent sub-areas and the center point of each sub-area is determined and distributed on the side of the base station. Due to the limited field of view of the drone detection equipment, the effective detection area of the drone needs to completely cover each sub-area to achieve coverage inspection (Figure 2). Therefore, it is necessary to preset the appropriate distance h between the target point passed by the drone and the center point of the inspection sub-area, so that the drone can complete the detection task of the center point and the area by passing through the preset target point. As shown in Figure 3, all the target points passed by the drone are distributed around the base station and the distance from the surface of the base station is h, then the drone inspection can be regarded as moving on the surface h away from the base station, that is, moving on the side of the cylinder. The preset target points it passes through are also regarded as distributed on the side of the cylinder.

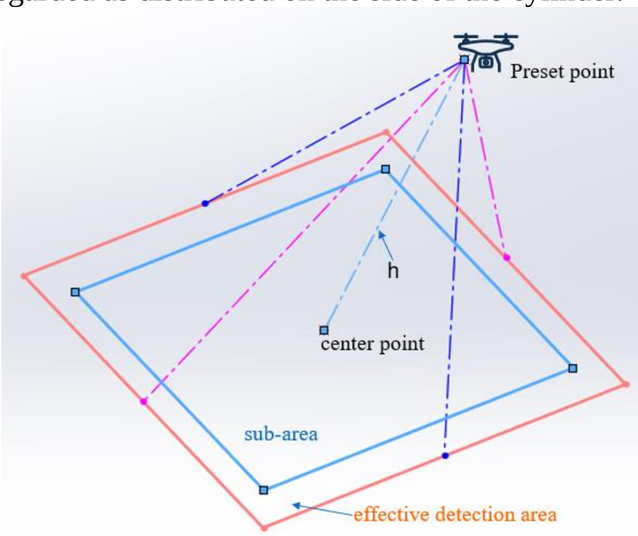

Figure. 2 Coverage of sub-areas by effective detection area

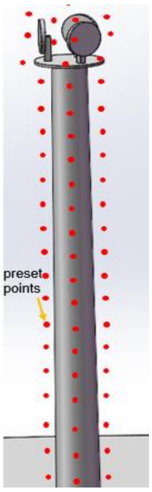

Figure. 3 Target points distributed around the base station model

In this paper, the inspected base station is assumed to be a regular cylinder with a diameter of 4 meters and a height of 40 meters. The circumference of the side of the cylinder where the drone is inspecting the base station is 22 meters, and the height is 40 meters. It is concentric with the cylindrical model of the base station. The distance h between the drone and the base station is 1.5 meters, the lateral field of view angle α is 60°, and the longitudinal field of view angle β is 120°. Then the lateral length A of the inspected area is

$$A = 2h \tan\left(\frac{\alpha}{2}\right) = 1.732\ m \tag{4}$$

The longitudinal length B of the detected area is

$$B = 2h \tan\left(\frac{\beta}{2}\right) = 5.196\ m \tag{5}$$

The area S of the effective detection area is

$$S = \mathrm{A} \cdot B = 8.999\ m^2 \tag{6}$$

For the drone to conduct full coverage inspection of the base station, the effective detection area of the drone needs to fully cover the sub-area. As shown in Figure 4, the rectangular side of the entire base station cylinder is divided into 64 sub-areas, with a bottom and height of 1.57 and 5m respectively, to ensure that the effective detection area fully covers it and determine its center point.

As shown in Figure 5, divide the rectangular side of the cylinder where the drone inspection path is located into 64 sub-areas. Each sub-area has a length of 2.75 meters and a width of 5 meters. The target point of each sub-area is determined to ensure that it completely overlaps with the effective detection area. (Figure 6). In addition, the drone nest is deployed at the midpoint of the bottom edge of the rectangle, and the drone can complete the inspection by passing through the set target point.

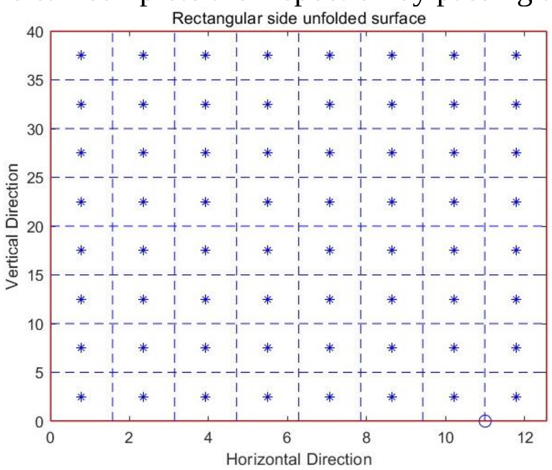

Figure. 4 Lateral expansion and sub-areas of the base station

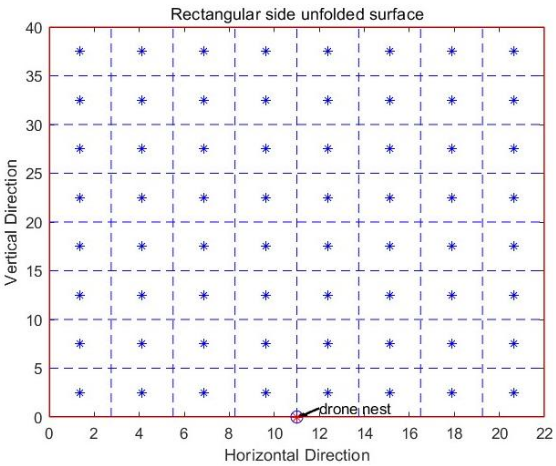

Figure. 5 The deployment and target points of the cylinder where the drone is inspected

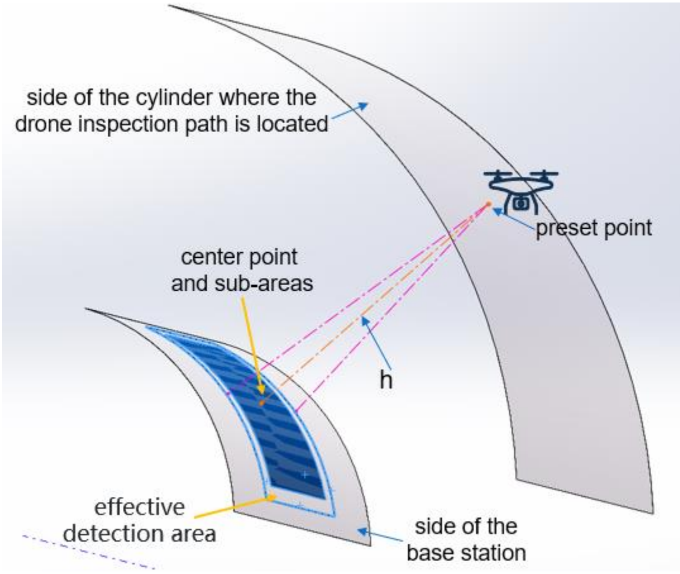

Figure. 6 Schematic diagram of drone inspection

2.2. Problem Analysis

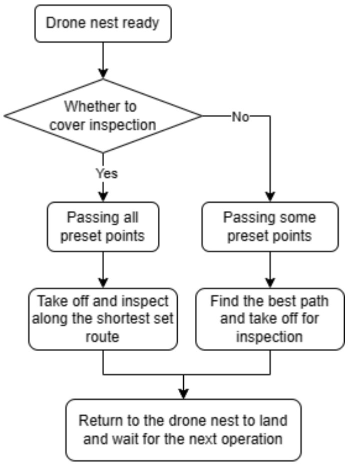

Figure. 7 Drone inspection flow chart

The inspection process of drones is shown in Figure 7. The inspection scheme is divided into comprehensive inspection and partial structural inspection. Comprehensive inspection requires drones to pass through all preset target points and cover all sub-areas. Partial structural inspection requires drones to pass through only some preset target points and cover key sub-areas and structures.

The planning of inspection routes requires the design of appropriate algorithms so that the inspection drones start from the drone nest, pass through the preset target points with the minimum path cost and return to the drone nest, and finally obtain the global optimal solution. The core problem is the Traveling Salesman Problem (TSP), that is, a traveling salesman starts from the starting point and goes to different destinations to sell goods. After traveling the least distance and reaching all destinations, he returns to the starting point, and the closed shortest path in which n target points are only passed once [9]. For the natural number set $\mathrm{N} = \{1,2,3 \cdots, \mathrm{n}\}$, there is a array $\mathrm{P(N)} = \{P_1, P_2, P_3 \cdots, P_n\}$ that minimizes:

$$Minimize \ \sum_{i=1}^{n-1} D(P_i\,, P_{i+1}) + D(P_n\,, P_1) \tag{7}$$

Where $D(P_i\,, P_{i+1})$ represents the distance from target point P_i to target point P_{i+1}, $D(P_n\,, P_1)$ represents the distance from the last visited target point P_n to the starting point P_1.

There are many algorithms that can solve the TSP problem (such as genetic algorithms, ant colony algorithms, simulated annealing algorithms). Among them, the simulated annealing algorithm (SA) is a randomized algorithm for global optimization problems. It draws on the physical process of metal annealing and simulates the slow cooling of metal after heating at high temperature to find the global optimal solution [10]. In the initial stage, the simulated annealing algorithm allows poor solutions to be accepted in order to escape the local optimum, and then gradually reduces this probability by lowering the "temperature", and eventually tends to converge to the global optimal solution. Since the simulated annealing algorithm is easy to implement and has strong flexibility, this paper uses this algorithm to find the optimal path.

2.3. Algorithm Implementation

The core idea of the simulated annealing algorithm is to find the global optimal solution by simulating the physical annealing process. That is, by controlling the temperature to gradually decrease, the probability of accepting a deteriorated solution is reduced, and in this process, a new solution is obtained through multiple iterations and continuously optimized. If the new solution is better than the current solution, the new solution is accepted and the search continues. If the new solution is worse than the current solution, the new solution is accepted with a certain probability according to the acceptance criterion, and then the search continues with this new solution until the termination condition is reached. The flowchart is shown in Figure 8. The following is a description of the steps of the simulated annealing algorithm to solve TSP:

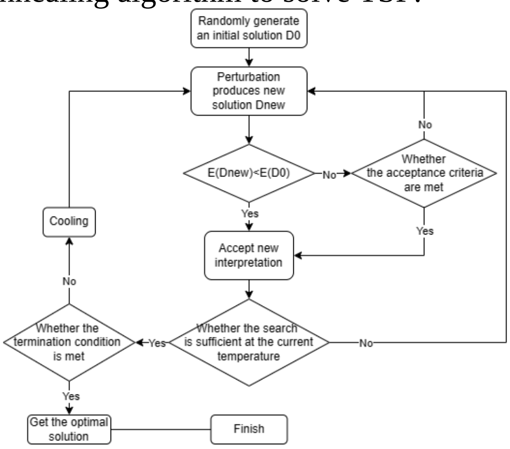

Figure. 8 SA algorithm flow chart

Initialization

Generate Initial Solution: Encode N target points as integers and generate a random arrangement (1 to N). Set this as the global optimal solution and calculate its objective function value (total path length).

Set Initial Temperature and End Condition: Set the initial temperature T, the temperature attenuation coefficient α $(0 < \alpha < 1)$, and the maximum iterations at each temperature $MaxIterN$.

Iterative Optimization

Generate New Solutions: Generate a new solution in the neighborhood of the current solution. Common methods include randomly swapping two target points, inserting one point into another position, or reversing a sequence of points.

Acceptance Criteria: Calculate the total path length difference

$$\Delta D = D_{new} - D_0 \tag{8}$$

where D_{new} is the new solution and D_0 is the current solution.

If $\Delta D < 0$ (better solution), accept the new solution.

If $\Delta D \geq 0$ (no better solution), accept the new solution with probability

$$P = exp(\frac{-\Delta E}{T}) \tag{9}$$

$$\Delta E = \frac{\Delta D}{D_0} \tag{10}$$

Where T is the current temperature.

After accepting the new solution, the new solution is taken as the current solution.

The following is the pseudo code of this process

```
    if f(Dnew)<=f(D0)
      D0=Dnew;
else
      delta=(f(Dnew)-f(D0))/f(D0);
      P=exp(-delta/T);
     if rand<=P                // rand is a random number in [0,1]
            D0=Dnew;
      end
end
```

Update Optimal Solution: If the current solution is better than the recorded optimal, update the optimal solution.

Lower the Temperature: Use the temperature decay formula to reduce the temperature

$$T = T * \alpha \tag{11}$$

Termination Condition: Stop the search when the maximum number of iterations is reached.

Output: Output the optimal solution and its path after the algorithm ends.

The flowchart of the complete simulated annealing algorithm to solve TSP is shown in Figure 9.

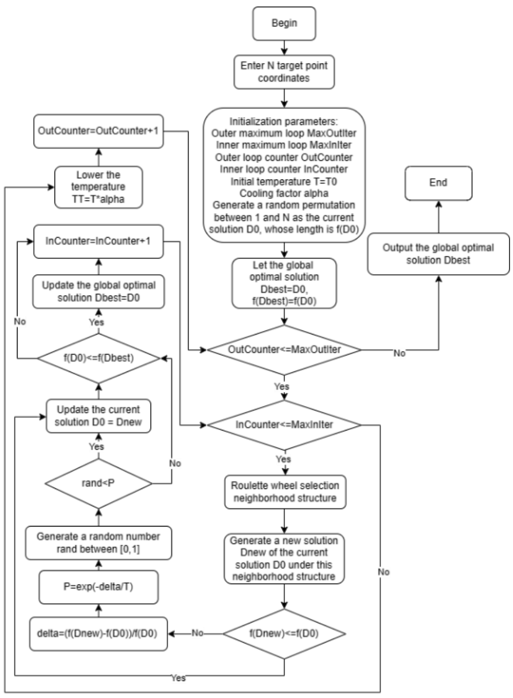

Figure 9 Flowchart of SA algorithm solving TSP

3. Experiment and Analysis

For the inspection scheme of this paper, it is necessary to design the shortest paths for comprehensive and partial structure inspections, respectively. MATLAB is used to implement the simulated annealing algorithm, build a simulation model, and draw the inspection path image.

3.1. Comprehensive Inspection Path Planning Simulation

Comprehensive inspection requires solving the TSP problem of all target points after the drone takes off from the drone nest. After multiple debugging and simulation runs, the algorithm simulation results are shown in Figure 10. The total length of the minimum inspection path is 210.456m. After about 250 iterations, the total length of the path can converge to a stable value (Figure 11). Thus, the algorithm can converge to the global optimal solution quickly.

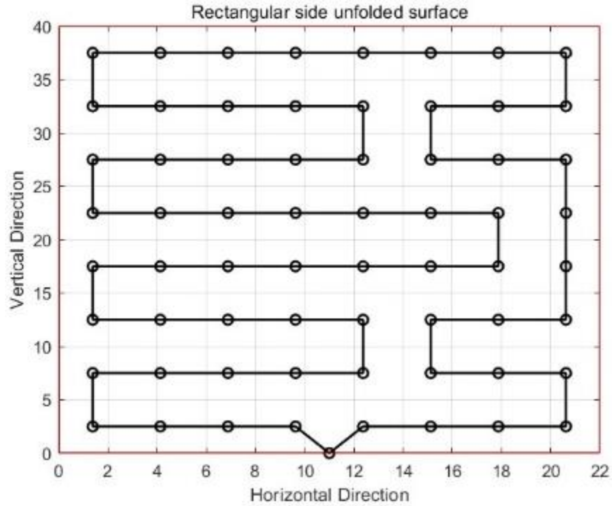

Figure. 10 Comprehensive inspection shortest inspection path simulation

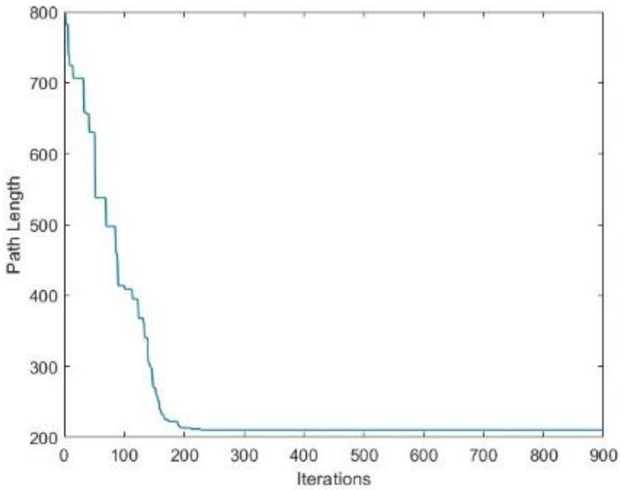

Figure .11 Iteration times graph

3.2. Simulation of Path Planning for Partial Structure Inspection

Partial structural inspections require the UAV to take off from the UAV nest and pass through some preset target points after the TSP problem. Randomly select 15 and 28 target points in different positions and perform multiple algorithm simulations. The simulation results of the path planning through 15 target points are shown in Figure 12. The shortest path is 109.133m. After about 10 iterations, the total path length can converge to a stable value (Figure 13). The simulation results of the path planning through 28 target points are shown in Figure 14. The shortest path is 153.935m. After about 150 iterations, the total path length can converge to a stable value (Figure 15)

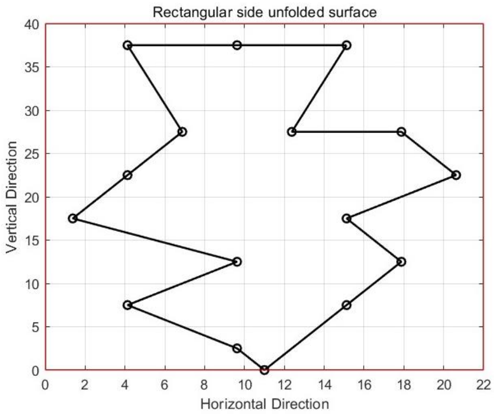

Figure. 12 Shortest inspection path simulation (15 points)

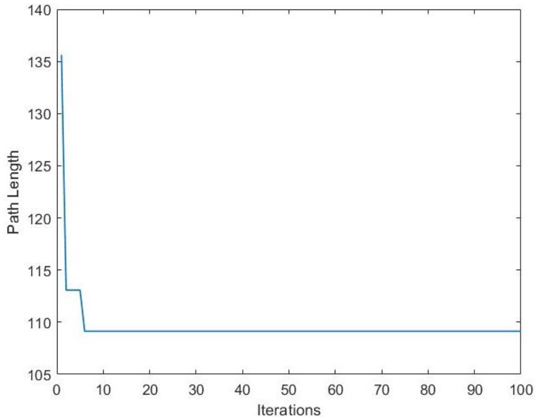

Figure. 13 Iteration times (15 points)

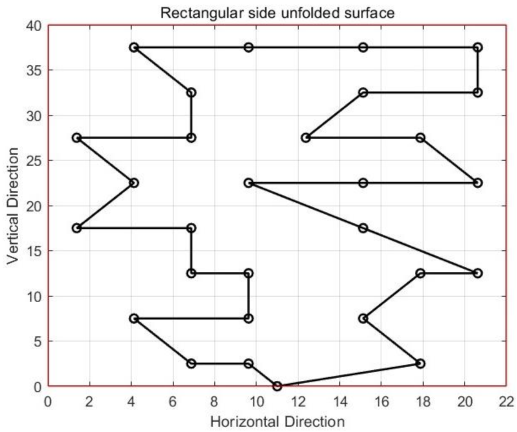

Figure. 14 Shortest inspection path simulation (28 points)

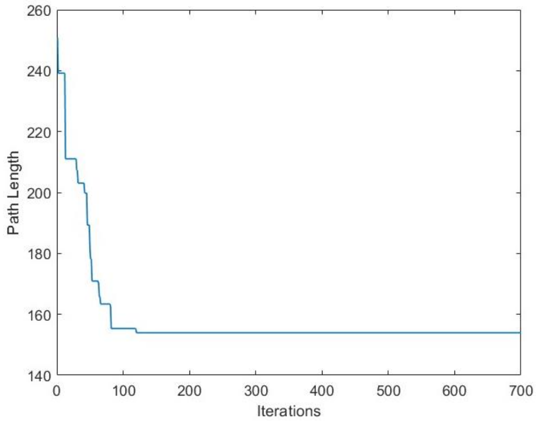

Figure. 15 Iteration times diagram (28 points)

3.3. Results and Discussion

The simulation results show that the automatic drone nest path planning based on the simulated annealing algorithm can find the global optimal solution in a short time, realize the full coverage and partial coverage inspection of the base station by drones, effectively improve the inspection efficiency of drones and reduce energy consumption. It is suitable for base station inspection scenarios that require unmanned and automatic conditions, such as remote areas and some locations that are difficult to reach manually. In general, the base station inspection scheme based on the automatic drone nest proposed in this paper provides a new idea for the unmanned inspection of communication base stations, effectively completes the inspection path planning task, and improves the automation of inspection. However, this paper limits the drone inspection path to the side of the cylinder and simplifies the three-dimensional scene into a two-dimensional scene for planning, which has certain limitations. Because in real scenes, instead of moving strictly along the side of the cylinder during inspection, drones need to adjust the distance appropriately to approach or move away from key structures. Therefore, future research should focus on optimizing these problems to improve the practicality of the scheme. In addition, the base station inspection scheme proposed in this paper needs to be verified in the actual scene, and improved and optimized in combination with actual data and feedback.

4. Conclusion

This paper proposes a mobile communication base station inspection scheme based on drone nests, designed to enhance the automation and efficiency of drone inspections. The approach involves establishing an inspection model, deploying target points, and applying the simulated annealing algorithm to solve the Traveling Salesman Problem (TSP) in the inspection path. The simulation experimental results show that the scheme can quickly plan the optimal inspection path under different requirements, thereby reducing energy consumption, and improving both efficiency and automation. This offers a novel approach to drone inspection and path planning using drone nests. However, the scheme still has limitations in terms of terrain around the base station and other external factors, and there is a discrepancy between the inspection scene model and real-world conditions. Future research should focus on further optimizing and improving this scheme, enhancing its practicality, and validating it in real-world scenarios.

References

[1] Xia Hua. Beijing has built more than 110,000 5G base stations to achieve precise signal coverage in key areas (2024, January 24). Beijing Daily.https://baijiahao.baidu.com/s?id=1788969238486458161&wfr=baike

[2] Statistical Communiqué Of The People'S Republic Of China On The 2023 National Economic And Social Development. China Statistics,2024, (03):4-21.

[3] LI Yuqiao. Research on Wind Turbine Blade Autonomous Inspection System based on Rotorcraft UAV. China University of Mining and Technology, 2021.

[4] Cui J, Zhang Y, Ma S, et al. Path planning algorithms for power transmission line inspection using unmanned aerial vehicles//2017 29th Chinese Control And Decision Conference (CCDC). IEEE, 2017: 2304-2309.

[5] Zhao F, Mo W, Hu Y, et al. Efficiently Optimizing Drone Nest Deployment for Transmission Line Inspection Based on Heuristic Algorithm//2023 China Automation Congress (CAC). IEEE, 2023: 9326-9331.

[6] Yang Zhi, LI Linjian, SHEN Junhao. Prospects for research and application of drone airport automatic patrol technology for oil and gas field gathering and transportation pipelines// The 33rd National Natural Gas Academic Annual Conference (2023) Proceedings (06 Comprehensive). China Petroleum Southwest Oil & Gas Field Company’s Communication and Information Technology Center, 2023:10.

[7] KONG Hui. Application and innovation of drones in environmental monitoring. Shanghai Light Industry,2024, (02):138-140.

[8] Gao Yangming. Research on the application of steel tower unmanned aerial vehicle inspection system. Telecommunications Information,2020, (04):37-39.

[9] Hahsler M, Hornik K. TSP-Infrastructure for the traveling salesperson problem. Journal of Statistical Software, 2007, 23(2): 1-21.

[10] Rutenbar R A. Simulated annealing algorithms: An overview. IEEE Circuits and Devices magazine, 1989, 5(1): 19-26.